

Deep Reinforcement Learning for Distributed Dynamic Power Allocation in Wireless Networks

Yasar Sinan Nasir and Dongning Guo

Department of Electrical Engineering and Computer Science

Northwestern University, Evanston, IL 60208.

Abstract

This work demonstrates the potential of deep reinforcement learning techniques for transmit power control in emerging and future wireless networks. Various techniques have been proposed in the literature to find near-optimal power allocations, often by solving a challenging optimization problem. Most of these algorithms are not scalable to large networks in real-world scenarios because of their computational complexity and instantaneous cross-cell channel state information (CSI) requirement. In this paper, a model-free distributed dynamic power allocation scheme is developed based on deep reinforcement learning. Each transmitter collects CSI and quality of service (QoS) information from several neighbors and adapts its own transmit power accordingly. The objective is to maximize a weighted sum-rate utility function, which can be particularized to achieve maximum sum-rate or proportionally fair scheduling (with weights that are changing over time). Both random variations and delays in the CSI are inherently addressed using deep Q-learning. For a typical network architecture, the proposed algorithm is shown to achieve near-optimal power allocation in real time based on delayed CSI measurements available to the agents. This work indicates that deep reinforcement learning based radio resource management can be very fast and deliver highly competitive performance, especially in practical scenarios where the system model is inaccurate and CSI delay is non-negligible.

I. INTRODUCTION

In emerging and future wireless networks, inter-cell interference management is one of the key technological challenges as access points (APs) become denser to meet ever-increasing demand on the capacity. A transmitter may increase its transmit power to improve its own data rate, but at the same time it may degrade some other links it interferes with. In order to optimize the system-level performance, transmit power control is a crucial technique that has been exploited since the first generation cellular networks [1]. Our goal here is to maximize an arbitrary weighted sum-rate objective, which achieves maximum sum-rate or proportionally fair scheduling as special cases. The NP-hardness of this problem is proven in [2].

A number of centralized and distributed optimization techniques were used to develop algorithms for reaching a suboptimal power allocation [1], [3]–[8]. We select two state-of-the-art algorithms as benchmarks. These are the weighted minimum mean square error (WMMSE) algorithm [3] and an iterative algorithm based on closed-form fractional programming (FP) [4]. In their generic form, both algorithms require full up-to-date cross-cell channel state information (CSI). Sun *et al.* [9] questioned the computational time required to run these algorithms and proposed a centralized *supervised learning* approach to train a faster deep neural network (DNN) that returns power allocation instantaneously. Their DNN achieves 90% or higher of the sum-rate achieved by the WMMSE algorithm. However, this approach still requires acquiring the full CSI. Another issue is that training DNN depends on a massive dataset of the WMMSE algorithm’s output for randomly generated CSI matrices. This dataset takes a significant amount of time to produce due to MMSE’s computational complexity. As the network gets larger, the total number of DNN’s input and output ports also increases, which raises questions on the scalability of the centralized solution of [9]. Furthermore, the success of supervised learning is highly dependent on the accuracy of the system model underlying the computed training data, which requires a new set of training data every time the system model or key parameters change.

Our main goal is to design a distributed algorithm to be employed by all transmitters to compute their

best power allocation in real time. Such a dynamic power allocation problem with time-varying channel conditions for a different system model and network setup was studied in [10] and the delay performance of the classical dynamic backpressure algorithm was improved by exploiting the stochastic Lyapunov optimization framework.

Our main contributions are summarized as follows.

- 1) We propose a new distributed dynamic power allocation algorithm based on recent advances in deep reinforcement learning, and in particular deep Q-learning [11]. The model-free nature of deep Q-learning [11] makes our algorithm robust to unpredictable changes in the wireless environment.
- 2) Since the complexity of its distributed framework does not depend on the network size, our algorithm is computationally scalable to networks that cover arbitrarily large geographical areas.
- 3) Our algorithm learns a policy that guides all links to adjust their power levels under important practical constraints such as delayed information exchange and incomplete cross-link CSI.
- 4) Unlike the supervised learning approach [9], there is no need to run a centralized algorithm to produce a large amount of training data. We use an applicable centralized network trainer approach that gathers local observations from all network agents. While a centralized training approach saves computational resources and converges faster, the training can also be carried out by individual or groups of agents separately.
- 5) We compare the reinforcement learning outcomes with state-of-the-art algorithms based on optimization techniques and show the scalability and the robustness of our algorithm using simulations. In the simulations, we model the channel variations inconsequential to the learning algorithm using Jakes' model [12]. We observe that in certain scenarios the proposed distributed algorithm even outperforms the centralized iterative algorithms introduced in [3], [4]. We also address practical constraints that are not included in [3], [4].

Applying Q-learning techniques on the power allocation problem has also been studied in [13]–[17]. The classical Q-learning technique has been proposed to reduce the interference in LTE-Femtocells in

[13], [14]. Unlike the deep Q-learning algorithm, the classical Q-learning algorithm builds a lookup table to represent the value of state-action pairs, so [13] and [14] represent the wireless environment using a discrete state set and limit the number of learning agents. Amiri *et al.* [15] have used cooperative Q-learning based power control to increase the QoS of users in femtocells without considering the channel variations. The deep Q-learning based power allocation to maximize the network objective has also been considered in [16], [17]. Similar to our approach, the work in [16], [17] is based on a distributed framework with a centralized training assumption, but the benchmark to evaluate the performance of their algorithm was a fixed power allocation scheme instead of state-of-the-art algorithms. Our approach to the state of wireless environment and the reward function is also novel and unique. Specifically, our approach addresses the stochastic nature of wireless environment as well as incomplete/delayed CSI, and arrives at highly competitive strategies quickly.

The remainder of this paper is organized as follows. We give the system model in Section II. In Section III, we formulate the dynamic power allocation problem and give our practical constraints on the local information. In Section IV, we first give an overview of deep Q-learning and then describe our algorithm. We give simulation results in Section V. We conclude with a discussion of possible future work in Section VI.

II. SYSTEM MODEL

We consider the classical power allocation problem in a network of n links. We assume that all transmitters and receivers are equipped with a single antenna. The model is often used to describe a mobile ad hoc network (MANET) [6]. The model has also been used to describe a simple cellular network with n APs, where each AP serves a single user device [4], [5]. Let $N = \{1, \dots, n\}$ denote the set of link indexes. We consider a fully synchronized time slotted system with slot duration T . For simplicity, we consider a single frequency band with flat fading. We adopt a block fading model to denote the downlink

channel gain from transmitter i to receiver j in time slot t as

$$g_{i \rightarrow j}^{(t)} = \left| h_{i \rightarrow j}^{(t)} \right|^2 \alpha_{i \rightarrow j}, \quad t = 1, 2, \dots \quad (1)$$

Here, $\alpha_{i \rightarrow j} \geq 0$ represents the large-scale fading component including path loss and log-normal shadowing, which remains the same over many time slots. We use Jakes' model [12] to express the small-scale Rayleigh fading component as a first-order complex Gauss-Markov process:

$$h_{i \rightarrow j}^{(t)} = \rho h_{i \rightarrow j}^{(t-1)} + e_{i \rightarrow j}^{(t)} \quad (2)$$

where $h_{i \rightarrow j}^{(0)} \sim \mathcal{CN}(0, 1)$ is circularly symmetric complex Gaussian (CSCG) with unit variance and the channel innovation process $e_{i \rightarrow j}^{(1)}, e_{i \rightarrow j}^{(2)}, \dots$ consists of independent and identically distributed CSCG random variables with distribution $\mathcal{CN}(0, 1 - \rho^2)$. The correlation $\rho = J_0(2\pi f_d T)$, where $J_0(\cdot)$ is the zero-order Bessel function of the first kind and f_d is the maximum Doppler frequency.

The received signal-to-interference-plus-noise ratio (SINR) of link i in time slot t is a function of the power allocation:

$$\gamma_i^{(t)}(\mathbf{p}) = \frac{g_{i \rightarrow i}^{(t)} p_i}{\sum_{j \neq i} g_{j \rightarrow i}^{(t)} p_j + \sigma^2} \quad (3)$$

where $\mathbf{p} = [p_1, \dots, p_n]^\top$ and σ^2 is the additive white Gaussian noise power spectral density (PSD) in receiver i . We assume the same noise PSD in all receivers without loss of generality. The downlink spectral efficiency of link i at time t can be expressed as:

$$C_i^{(t)}(\mathbf{p}) = \log \left(1 + \gamma_i^{(t)}(\mathbf{p}) \right). \quad (4)$$

The transmit power of transmitter i in time slot t is denoted as $p_i^{(t)}$. We denote the power allocation of the network in time slot t as $\mathbf{p}^{(t)} = [p_1^{(t)}, \dots, p_n^{(t)}]^\top$. With dynamically allocated power $\mathbf{p}^{(t)}$, the spectral efficiency is then $C_i^{(t)}(\mathbf{p}^{(t)})$ in time slot t .

III. DYNAMIC POWER CONTROL

We are interested in maximizing a generic weighted sum-rate objective function. Specifically, the dynamic power allocation problem in slot t is formulated as

$$\underset{\mathbf{p}}{\text{maximize}} \quad \sum_{i=1}^n w_i^{(t)} \cdot C_i^{(t)}(\mathbf{p}) \quad (5)$$

$$\text{subject to} \quad 0 \leq p_i \leq P_{\max}, \quad \forall i \in N$$

where $w_i^{(t)}$ is the given nonnegative weight of link i in time slot t , and P_{\max} is the maximum power a transmitter can emit. Hence, the dynamic power allocator has to solve an independent problem in the form of (5) at the beginning of every time slot. In time slot t , the optimal power allocation solution is denoted as $\mathbf{p}^{(t)}$. Problem (5) is in general non-convex and its NP-hardness was shown in [2].

We consider two different objectives: sum-rate maximization and proportional fair scheduling. In the former case, $w_i^{(t)} = 1$ for all i and t . In the latter case, the weights vary in a controlled manner to ensure fairness [8], [18]. First, at the end of time slot t , receiver i computes its weighted average spectral efficiency as

$$\bar{C}_i^{(t)} = \beta \cdot C_i^{(t)}(\mathbf{p}^{(t)}) + (1 - \beta) \bar{C}_i^{(t-1)} \quad (6)$$

where $\beta \in (0, 1]$ is used to control the impact of history. User i updates its link weight with the following equation:

$$w_i^{(t+1)} = \frac{1}{\bar{C}_i^{(t)}}. \quad (7)$$

If each agent follows this weight update scheme, the power allocation algorithm is going to maximize the sum of log-average spectral efficiency [18], i.e.,

$$\sum_{i \in N} \log \bar{C}_i^{(t)}, \quad (8)$$

where a user's long-term average throughput is proportional to its long-term channel quality in some sense and it is typically allocated more resources when its channel quality is better.

We use two popular (suboptimal) power allocation algorithms as benchmarks. These are the WMMSE algorithm [3] and the FP algorithm [4]. Both are centralized and iterative in their generic form. A detailed explanation and pseudo code of WMMSE algorithm is given in [9, Fig. 2]. In the next section, we describe the FP algorithm for completeness.

A. The FP Algorithm

Shen and Yu [4] propose to use the Lagrangian dual reformulation approach [4, Proposition 2] to take the SINR term described in (3) out of the logarithm. For ease of notation, we drop the time index (t) to write the power control problem in an arbitrary slot:

$$\begin{aligned} & \underset{\mathbf{p}, \gamma}{\text{maximize}} \quad \sum_{i \in N} w_i (\log(1 + \gamma_i) - \gamma_i) + \frac{w_i (1 + \gamma_i) g_{i \rightarrow i} p_i}{\sum_{j \in N} g_{j \rightarrow i} p_j + \sigma^2} \\ & \text{subject to} \quad 0 \leq p_i \leq P_{\max}, \quad \forall i \in N \end{aligned} \quad (9)$$

where γ denotes the set of auxiliary variables $(\gamma_i)_{i=1}^n$. If (p_i) are fixed, the optimal γ_i is obtained as,

$$\gamma_i^* = \frac{g_{i \rightarrow i} p_i}{\sum_{j \neq i} g_{j \rightarrow i} p_j + \sigma^2}, \quad \forall i \in N. \quad (10)$$

Hence (9) is equivalent to (5). To treat the fractional term in the objective in (9), Shen and Yu applied a quadratic transform [4, Theorem 1] to rewrite the fractional term in (9) as:

$$\begin{aligned} f_q(\mathbf{p}, \gamma, \mathbf{y}) &= \sum_{i \in N} 2y_i \sqrt{w_i (1 + \gamma_i) g_{i \rightarrow i} p_i} \\ &\quad - \sum_{i \in N} y_i^2 \left(\sum_{j \in N} g_{j \rightarrow i} p_j + \sigma^2 \right) \end{aligned} \quad (11)$$

where \mathbf{y} is the set of auxiliary variables $(y_i)_{i=1}^n$. It is easy to see that, for fixed γ and \mathbf{p} ,

$$y_i^* = \frac{\sqrt{w_i (1 + \gamma_i) g_{i \rightarrow i} p_i}}{\sum_{j \in N} g_{j \rightarrow i} p_j + \sigma^2}, \quad \forall i \in N \quad (12)$$

achieves the maximum of $f_q(\mathbf{p}, \gamma, \mathbf{y})$, which becomes the fractional term in (9).

The FP algorithm as described in Algorithm 1 basically iteratively solve for the optimal \mathbf{y} , γ , and \mathbf{p} by holding the other two sets of variables fixed.

Algorithm 1 Pseudo code of the closed-form FP [4]

1: Initialize \mathbf{p} in pseudo-random fashion s.t. $0 \leq p_i \leq P_{\max}$, $\forall i$;

2: Initialize γ by (10);

3: **repeat**

4: Update \mathbf{y} by (12) for fixed (γ, \mathbf{p}) ;

5: Update γ by (10) for fixed (\mathbf{y}, \mathbf{p}) ;

6: Update \mathbf{p} for fixed (γ, \mathbf{y}) as:

$$p_i^* = \min \left\{ P_{\max}, \frac{y_i^2 w_i (1 + \gamma_i) g_{i \rightarrow i}}{\sum_{j \in N} y_j^2 g_{i \rightarrow j}} \right\}, \quad \forall i \in N. \quad (13)$$

7: **until** numerical convergence of the objective

8: **return** \mathbf{p}

B. Delayed Information Exchange

The WMMSE and FP algorithms are both centralized and require full cross-link CSI. The centralized mechanism is suitable for a stationary environment with no fast fading and quite slowly varying weights in the utility function. For a network with non-stationary environment, it is infeasible to instantaneously collect all CSI over a large network.

It is fair to assume that the feedback delay T_{fb} from a receiver to its corresponding transmitter is much smaller than T , so the prediction error due to the feedback delay is neglected. Therefore, once receiver i completes a direct channel measurement, we assume that it is also available at the transmitter i . We also neglect the measurement errors caused by the imperfections of physical instruments.

For the centralized approach, once a link acquires the CSI of its direct channel and all other interfering channels to its receiver, passing this information to a central controller is another burden. This is typically resolved using a backhaul network between the APs and the central controller. There will be additional delays through the backhaul network. As a result, the CSI of cross links is usually delayed or completely outdated. Furthermore, the central controller can only return the optimal power allocation as the iterative

algorithm converges, which is another limitation on the scalability.

Our goal is to design a scalable algorithm, so we limit the information exchange between nearby transmitters. We define two neighborhood sets for every $i \in N$: Let the set of transmitters whose received SNR at receiver i was above a certain threshold η during the past time slot $t - 1$ be denoted as

$$I_i^{(t)} = \left\{ j \in N, j \neq i \mid g_{j \rightarrow i}^{(t-1)} p_j^{(t-1)} > \eta \sigma^2 \right\}. \quad (14)$$

Let the set of receiver indexes whose SNR from transmitter i was above a threshold in slot $t - 1$ be denoted as

$$O_i^{(t)} = \left\{ k \in N, k \neq i \mid g_{i \rightarrow k}^{(t-1)} p_i^{(t-1)} > \eta \sigma^2 \right\}. \quad (15)$$

From link i 's viewpoint, $I_i^{(t)}$ represents the set of “interferers”, whereas $O_i^{(t)}$ represents the set of the “interfered”.

We next discuss the local information a transmitter possesses at the beginning of time slot t . First, we assume that transmitter i learns via receiver feedback the direct downlink channel gain, $g_{i \rightarrow i}^{(t)}$. Further, transmitter i also learns the current total received interference-plus-noise power at receiver i before the global power update, i.e., $\sum_{j \in N, j \neq i} g_{j \rightarrow i}^{(t)} p_j^{(t-1)} + \sigma^2$ (as a result of the new gains and the yet-to-be-updated powers). In addition, by the beginning of slot t , receiver i has informed transmitter i of the received power from every interferer $j \in I_i^{(t)}$, i.e., $g_{j \rightarrow i}^{(t)} p_j^{(t-1)}$. These measurements can only be available at transmitter i just before the beginning of slot t . Hence, in the previous slot $t - 1$, receiver i also informs transmitter i of the outdated versions of these measurements to be used in the information exchange process performed in slot $t - 1$ between transmitter i and its interferers. To clarify, as shown in Fig. 1, transmitter i has sent the following outdated information to interferer $j \in I_i^{(t)}$ in return for $w_j^{(t-1)}$ and $C_j^{(t-1)}$:

- the weight of link i , $w_i^{(t-1)}$,
- the spectral efficiency of link i computed from (4), $C_i^{(t-1)}$,
- the direct gain, $g_{i \rightarrow i}^{(t-1)}$,
- the received interference power from transmitter j , $g_{j \rightarrow i}^{(t-1)} p_j^{(t-1)}$,

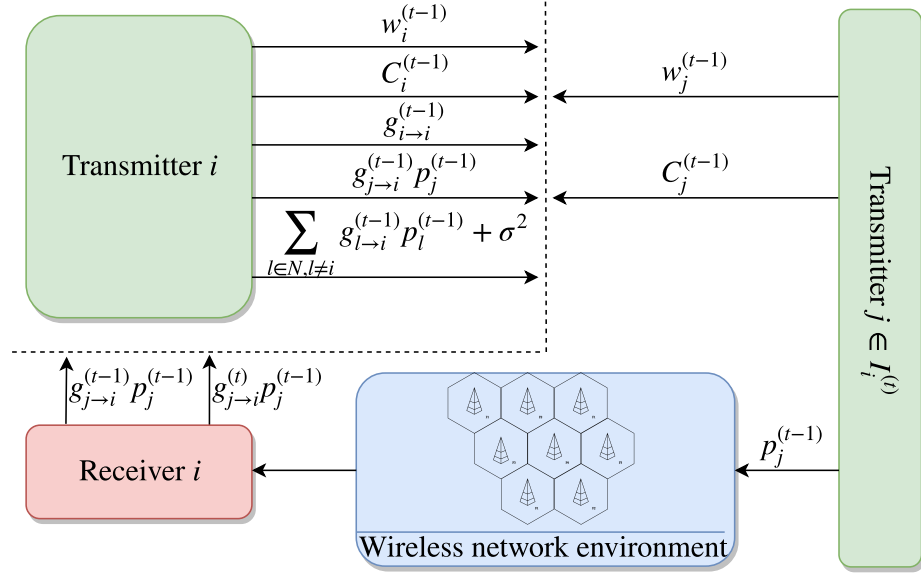


Fig. 1: The information exchange between transmitter i and interferer $j \in I_i^{(t)}$ in time slot $t - 1$. Note that transmitter i obtains $g_{j \rightarrow i}^{(t-1)} p_j^{(t-1)}$ by the end of slot $t - 1$, but it is not able to deliver this information to interferer j before the beginning of slot t due to additional delays through the backhaul network.

- the total interference-plus-noise power at receiver i , i.e., $\sum_{l \in N, l \neq i} g_{l \rightarrow i}^{(t-1)} p_l^{(t-1)} + \sigma^2$.

As assumed earlier, these measurements are accurate, where the uncertainty about the current CSI is entirely due to the latency of information exchange (one slot). By the same token, from every interfered $k \in O_i^{(t)}$, transmitter i also obtains k 's items listed above.

IV. DEEP REINFORCEMENT LEARNING FOR DYNAMIC POWER ALLOCATION

A. Overview of Deep Q -Learning

A reinforcement learning agent learns its best policy from observing the rewards of trial-and-error interactions with its environment over time [19], [20]. Let S denote a set of possible states and A denote a discrete set of actions. Assuming discrete time steps, the agent observes the state of its environment, $s^{(t)} \in S$ at time step t . It then takes an action $a^{(t)} \in A$ according to a certain policy π . The policy $\pi(s, a)$ is the probability of taking action a conditioned on the current state being s . The policy function must satisfy $\sum_{a \in A} \pi(s, a) = 1$.

Once the agent takes an action $a^{(t)}$, its environment moves from the current state $s^{(t)}$ to the next state $s^{(t+1)}$. As a result of this transition, the agent gets a reward $r^{(t+1)}$ that characterizes its benefit from taking action $a^{(t)}$ at state $s^{(t)}$. This scheme forms an experience at time t : $(s^{(t)}, a^{(t)}, r^{(t+1)}, s^{(t+1)})$.

The Q-learning algorithm is a well-known model-free algorithm for computing an optimal policy π that maximizes the expectation of the future cumulative discounted reward. The future cumulative discounted reward at time t is

$$R^{(t)} = \sum_{\tau=0}^{\infty} \gamma^{\tau} r^{(t+\tau+1)} \quad (16)$$

where $\gamma \in (0, 1]$ is the discount factor for future rewards. In the stationary setting, we define a Q-function associated with a certain policy π as the expected future cumulative discounted reward once action a is taken under state s [21], i.e.,

$$Q^{\pi}(s, a) = \mathbb{E}_{\pi} [R^{(t)} | s^{(t)} = s, a^{(t)} = a]. \quad (17)$$

As an action value function, the Q-function satisfies a Bellman equation [22] derived as

$$Q^{\pi}(s, a) = \mathcal{R}(s, a) + \gamma \sum_{s' \in S} \mathcal{P}_{ss'}^a \left(\sum_{a' \in A} \pi(s', a') Q^{\pi}(s', a') \right) \quad (18)$$

where $\mathcal{R}(s, a) = \mathbb{E} [r^{(t+1)} | s^{(t)} = s, a^{(t)} = a]$ is the expected reward of taking action a at state s , and $\mathcal{P}_{ss'}^a = \Pr(s^{(t+1)} = s' | s^{(t)} = s, a^{(t)} = a)$ is the transition probability from given state s to state s' with action a . From the fixed-point equation (18), the value of (s, a) can be recovered from all values of $(s', a') \in S \times A$. It has been proved that some iterative approaches such as Q-learning algorithm efficiently converges to the action value function (17) [21].

The Q-learning algorithm searches an optimal policy denoted as π^* . Clearly, $\pi^*(s, a)$ is equal to 1 for the action that maximizes the expected future cumulative discounted reward given the state s [21]. From (18), the optimal Q-function associated with the optimal policy becomes

$$Q^*(s, a) = \mathcal{R}(s, a) + \gamma \sum_{s' \in S} \mathcal{P}_{ss'}^a \max_{a'} Q^*(s', a'). \quad (19)$$

The classical Q-learning algorithm constructs a lookup table, $q(s, a)$, as a surrogate of the optimal Q-function. Once this lookup table is randomly initialized, the agent takes actions according to the ϵ -greedy policy for each time step. The ϵ -greedy policy implies that with probability $1 - \epsilon$ the agent takes the action a^* that gives the maximum lookup table value for a given current state, whereas it picks a random action with probability ϵ to avoid getting stuck at non-optimal policies [11]. After acquiring a new experience as a result of the taken action, the Q-learning algorithm updates a corresponding entry of the lookup table according to:

$$\begin{aligned} q(s^{(t)}, a^{(t)}) &\leftarrow (1 - \alpha)q(s^{(t)}, a^{(t)}) \\ &+ \alpha \left(r^{(t+1)} + \gamma \max_{a'} q(s^{(t+1)}, a') \right) \end{aligned} \quad (20)$$

where $\alpha \in (0, 1]$ is the learning rate [21].

The classical Q-learning algorithm shows high performance with small state and action spaces, which is not the case for the power control problem at hand. As problem size increases, the classical Q-learning algorithm fails because of two main reasons: many states are rarely visited and the storage of lookup table in (20) becomes impractical [23]. These issues can be solved with deep reinforcement learning, e.g., deep Q-learning [11]. A deep neural network called deep Q-network (DQN) is used to estimate the Q-function in lieu of a lookup table. The DQN can be expressed as $q(s, a, \theta)$, where θ is its weights. The essence of DQN is that the function $q(\cdot, \cdot, \theta)$ is completely determined by θ . As such, the task of finding the best Q-function in a functional space of uncountably many dimensions is reduced to searching the best real-valued weight vector θ of finite dimensions. Similar to the classical Q-learning, the agent collects experiences with its interaction with the environment. The agent or the network trainer forms a data set D by collecting the experiences until time t in the form of (s, a, r', s') . As the “quasi-static target network” method [11] imply, we define two DQNs: the target DQN with weights $\theta_{\text{target}}^{(t)}$ and the train DQN with weights $\theta_{\text{train}}^{(t)}$. $\theta_{\text{target}}^{(t)}$ is updated once per T_u steps with $\theta_{\text{train}}^{(t)}$. From the “experience replay” [11], the least

squares loss of train DQN for a random mini-batch $D^{(t)}$ at time t is

$$L\left(\boldsymbol{\theta}_{\text{train}}^{(t)}\right) = \sum_{(s,a,r',s') \in D^{(t)}} \left(y_{DQN}^{(t)}(r', s') - q\left(s, a; \boldsymbol{\theta}_{\text{train}}^{(t)}\right) \right)^2 \quad (21)$$

where the target is

$$y_{DQN}^{(t)}(r', s') = r' + \lambda \max_{a'} q\left(s', a'; \boldsymbol{\theta}_{\text{target}}^{(t)}\right). \quad (22)$$

Finally, we assume that each time step the stochastic gradient descent algorithm that minimizes the loss function (21) is used to train the mini-batch $D^{(t)}$. The stochastic gradient descent returns the new weights of train DQN using the gradient computed from just few samples of the dataset and surprisingly converges to good set of weights quickly [24].

B. Proposed Deep Reinforcement Learning for Distributed Dynamic Power Allocation

As depicted in Fig. 2, our algorithm is a distributed multi-agent deep reinforcement learning scheme where each transmitter serves as an agent. Similar to [17], we use a centralized training and distributed execution framework. At the beginning of time slot t , agent i takes action $a_i^{(t)}$ as a function of $s_i^{(t)}$ based on the current decision policy. All agents are synchronized and take their actions at the same time. Prior to taking action, agent i has observed the effect of the past actions of its neighbors on its current state, but it has no knowledge of $a_j^{(t)}$, $\forall j \neq i$. From the past experiences, agent i is able to acquire an estimation of what is the impact of its own actions on future actions of its neighbors, and it can determine a policy that maximizes its discounted expected future reward with the help of deep Q-learning.

The proposed DQN is a fully-connected deep neural network with a similar architecture shown in [25, Fig. 3]. The DQN's total number of input and output ports equal to the cardinality of the state set and the action set, respectively. Each DQN output gives an estimate of the Q-function with given state input and the corresponding action output. The DQN used in our simulations has three hidden layers, and its size is considerably small compared to the neural network used in [9]. We later give the choice of DQN's activation function and its hyper-parameters in Section V-A.

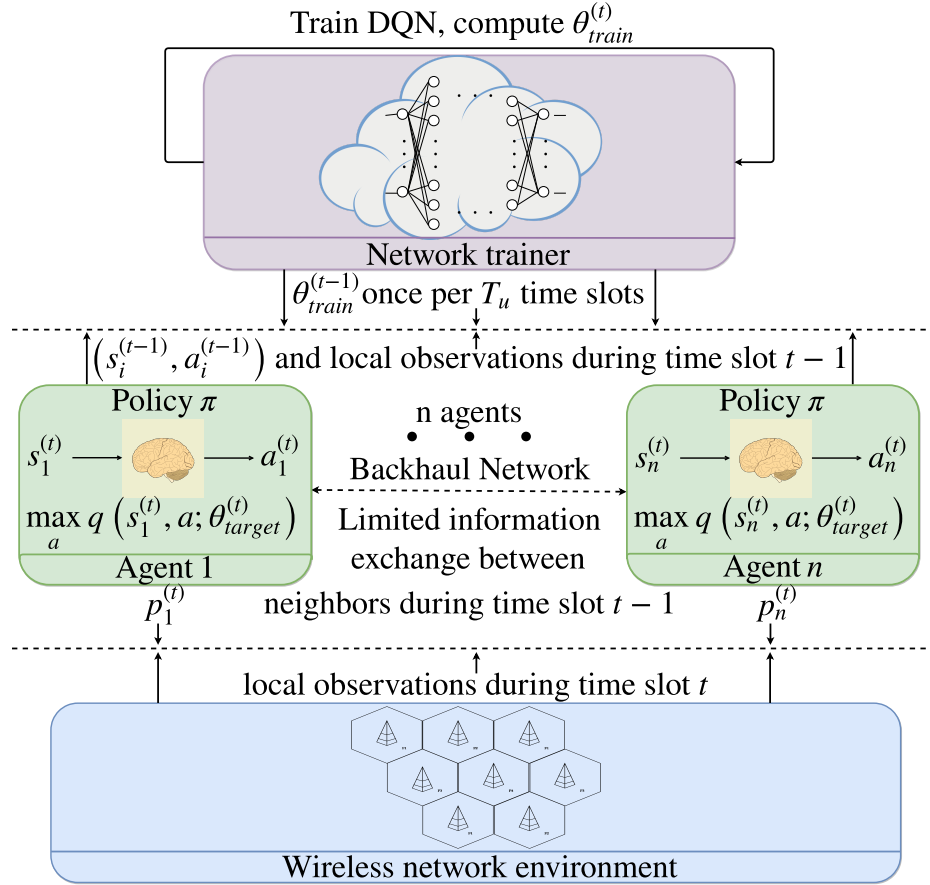


Fig. 2: Illustration of the proposed deep reinforcement learning for distributed dynamic power allocation.

Each agent i has the same copy of DQN with weights $Q_{\text{target}}^{(t)}$ at time slot t . The centralized network trainer trains a single DQN by using the experiences gathered from all agents. This significantly reduces the amount of memory and computational resources required during the training. Each time slot, if the training of DQN is not over, the network trainer randomly selects a mini-batch $D^{(t)}$ of M_b experiences from an experience-replay memory of nM_m samples, where n is the total number of agents. The experience-replay memory is a FIFO queue, i.e., a new experience replaces the oldest experience in the queue [26], and at time slot t the most recent experience from agent i is $(s_i^{(t-2)}, a_i^{(t-2)}, r_i^{(t-1)}, s_i^{(t-1)})$ because of the propagation delay between agent i and the network trainer. Once the network trainer picks $D^{(t)}$, it updates the weights of its train DQN once per time slot with a suitable optimizer such as stochastic gradient descent [24] that minimizes the loss in (21). Once per T_u time slots, the network trainer broadcasts current weights of its train DQN. The new weights are available at the agents after one time slot, again,

due to the propagation delay. Once the training converges, the network trainer leaves the network and the resources that carried the training through can be used elsewhere.

C. States

In Section III-B, we introduced the neighborhood concept and discussed the local information available at transmitter (agent) i at the beginning of time slot t . This local information is going to determine the current state of the environment $s_i^{(t)}$.

Because of the fixed input structure of the DQN, we regulate the cardinality of the interferer and interfered sets $(I_i^{(t)}, O_i^{(t)})$. Hence, we define the regulated interferer and interfered neighborhood sets at time slot t denoted as $\bar{I}_i^{(t)}$ and $\bar{O}_i^{(t)}$, respectively. We set $|\bar{I}_i^{(t)}| = |\bar{O}_i^{(t)}| = c$, where $c > 0$ is the restriction on the number of interferers and interfereds the AP communicating with. At the beginning of time slot t , agent i sorts its interferers by current received power from interferer $j \in I_i^{(t)}$ at receiver i , i.e., $g_{j \rightarrow i}^{(t)} p_j^{(t-1)}$. If $|I_i^{(t)}| < c$, agent i adds $|I_i^{(t)}| - c$ virtual noise agents to $I_i^{(t)}$. A virtual noise agent is just a placeholder with an arbitrary negative weight and spectral efficiency. Its downlink and interfering channel gains are taken as zero. After adding virtual noise agents (if needed), agent i takes first c interferers to form $\bar{I}_i^{(t)}$. For the interfered neighbors, agent i follows a similar procedure, but this time sorting criteria is the share of agent i on the interference at receiver $k \in O_i^{(t)}$, i.e.,

$$\frac{g_{i \rightarrow k}^{(t-1)} p_i^{(t-1)}}{\sum_{j \in N, j \neq k} g_{j \rightarrow k}^{(t-1)} p_j^{(t-1)} + \sigma^2}.$$

Now, we can describe the state of agent i at time slot t , i.e., $s_i^{(t)}$, by dividing it into three main feature groups as:

- 1) Local Information: First, agent i feeds DQN with its transmit power during previous time slot $t-1$, i.e., $p_i^{(t-1)}$. Then, this is followed by the most recent indicators of its potential contribution on the network objective (5): $\frac{1}{w_i^{(t)}}$ and $C_i^{(t-1)}$. Its last four indexes are the last two measurements of its direct downlink channel and the total interference-plus-noise power at receiver i : $g_{i \rightarrow i}^{(t)}$, $g_{i \rightarrow i}^{(t-1)}$,

$\sum_{j \in N, j \neq i} g_{j \rightarrow i}^{(t)} p_j^{(t-1)} + \sigma^2$, and $\sum_{j \in N, j \neq i} g_{j \rightarrow i}^{(t-1)} p_j^{(t-2)} + \sigma^2$. Hence, seven input ports are reserved for this feature group.

2) Interferer Neighbors: This feature group lets agent i to observe the interference from its neighbors to receiver i and what is the contribution of these interferers on the objective (5). For each interferer $j \in \bar{I}_i^{(t)}$, three input ports are reserved for $g_{j \rightarrow i}^{(t)} p_j^{(t-1)}$, $\frac{1}{w_j^{(t-1)}}$, $C_j^{(t-1)}$. In addition to the current interferers, agent i also includes the ones from the previous time slot. Similarly, for each interferer $j' \in \bar{I}_i^{(t-1)}$, three input ports are reserved for $g_{j' \rightarrow i}^{(t-1)} p_{j'}^{(t-2)}$, $\frac{1}{w_{j'}^{(t-2)}}$, $C_{j'}^{(t-2)}$. This makes a total of $6c$ state indexes reserved for the interferers.

3) Interfered Neighbors: Finally, agent i uses the feedback from its interfered neighbors to get a sense of its interference to nearby receivers and the contribution of them on (5). Note that if agent i was inactive during previous time slot, i.e., $p_i^{(t-1)} = 0$, then $O_i^{(t-1)} = \emptyset$. For this case, if we ignore the history and directly consider the current interfered neighbor set, corresponding state indexes will be useless. We solve this issue by defining time slot t'_i which is the last time slot agent i was active. The agent i carries the feedback from interfered $k \in \bar{O}_i^{(t'_i)}$. We also pay attention to the fact that if $t'_i < t - 1$, interfered k has no knowledge of $g_{i \rightarrow k}^{(t-1)}$, but it is still able to send its local information to agent i . After this remark, agent i reserves four indexes of its state set for each interfered $k \in \bar{O}_i^{(t'_i)}$ as $g_{k \rightarrow k}^{(t-1)}$, $\frac{1}{w_k^{(t-1)}}$, $C_k^{(t-1)}$, and

$$\frac{g_{i \rightarrow k}^{(t'_i)} p_i^{(t'_i)}}{\sum_{j \in N, j \neq k} g_{j \rightarrow k}^{(t-1)} p_j^{(t-1)} + \sigma^2}.$$

This makes a total of $4c$ indexes of the state set reserved for the interfered neighbors.

D. Actions

Unlike taking discrete steps on the previous transmitted power level (see, e.g., [16]), we use discrete power levels taken between 0 and P_{\max} . This way of approaching the problem could increase the number

of DQN output ports compared to [16], but it will increase the robustness of the learning algorithm. Suppose we have $|A| > 1$ discrete power levels. Then, the action set is given by

$$A = \left\{ 0, \frac{P_{\max}}{|A| - 1}, \frac{2P_{\max}}{|A| - 1}, \dots, P_{\max} \right\}. \quad (23)$$

Agent i is only allowed to pick an action $a_i(t) \in A$ to update its power strategy at time slot t .

E. Reward Function

From Fig. 2, the network trainer computes the reward function of every agent $i \in N$ for the next time slot $t + 1$, i.e., $r_i^{(t+1)}$, by using the state action pairs and local observations gathered from all agents.

The criterion the reward function takes into account should be how the action of agent i through time slot t , i.e., $p_i^{(t)}$, affects the weighted sum-rate of its own and its future interfered neighbors $O_i^{(t+1)}$. During the time slot $t + 1$, for all agent $i \in N$, the network trainer calculates the spectral efficiency of each link $k \in O_i^{(t+1)}$ without the interference from transmitter i as

$$C_{k-i}^{(t)} = \log \left(1 + \frac{g_{k \rightarrow k}^{(t)} p_k^{(t)}}{\sum_{j \neq i, k} g_{j \rightarrow k}^{(t)} p_j^{(t)} + \sigma^2} \right). \quad (24)$$

Note that the network trainer computes the term $\sum_{j \neq i, k} g_{j \rightarrow k}^{(t)} p_j^{(t)} + \sigma^2$ in (24) by simply subtracting $g_{i \rightarrow k}^{(t)} p_i^{(t)}$ from the total interference-plus-noise power at receiver k in time slot t . As we assumed in Section III-B, since transmitter $i \in I_k^{(t+1)}$, its interference to link k in slot t , i.e., $g_{i \rightarrow k}^{(t)} p_i^{(t)} > \eta \sigma^2$, is accurately measurable by receiver k and has been delivered to the network trainer.

We next define the externality link i causes to link k , i.e., the price charged to link i for generating interference to link k [6], in time slot t as

$$\pi_{i \rightarrow k}^{(t)} = w_k^{(t)} \left(C_{k-i}^{(t)} - C_k^{(t)} \right). \quad (25)$$

Then, the reward function of agent $i \in N$ at time slot $t + 1$ is defined as

$$r_i^{(t+1)} = w_i^{(t)} C_i^{(t)} - \sum_{k \in O_i^{(t+1)}} \pi_{i \rightarrow k}^{(t)}. \quad (26)$$

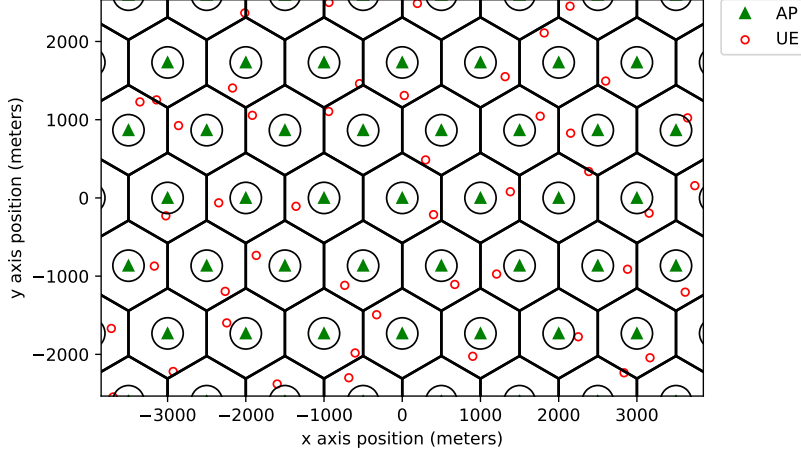


Fig. 3: A network configuration example with $R = 500$ m and $r = 200$ m.

The reward of agent i consists of two main components: its contribution on the network objective (5) and the penalty caused by sum-externality to its interfered neighbors. Suppose $p_i^{(t)} = P_{\max}$, then the penalty of agent i is maximized. On the contrary, if agent i transmits nothing, its reward for the next time slot is simply zero.

V. SIMULATION RESULTS

A. Simulation Setup

To begin with, we consider n links on n homogeneously deployed cells, where we later choose n to be between 19 and 100. Transmitter i is located at the center of cell i and receiver i is located randomly within the cell. The half transmitter-to-transmitter distance is denoted as R and it is between 100 and 1000 meters. We also define an inner region of radius r where no receiver is allowed to be placed. We set the r value between 10 and $R - 1$ meters. Receiver i is placed randomly according to a uniform distribution on the area between out of the inner region of radius r and the cell boundary. Fig. 3 shows a network configuration example.

We set P_{\max} , i.e., the maximum transmit power level of transmitter i , to 38 dBm over 10 MHz frequency band which is fully reusable across all links. The distance dependent path loss between all transmitters and receivers is simulated by $120.9 + 37.6 \log_{10}(d)$ (in dB), where d is transmitter-to-receiver distance in

km. This path loss model is compliant with the LTE standard [27]. The log-normal shadowing standard deviation is taken as 8 dB. The AWGN power σ^2 is -114 dBm. Similar to [28], if the received SINR is greater than 30 dB, it is capped at 30 dB in the calculation of spectral efficiency by (4). This is to account for typical limitations of digital processing. In addition to these parameters, we take the period of the time-slotted system T to be 20 ms. Unless otherwise stated, the maximum Doppler frequency f_d is 10 Hz and identical for all receivers.

We next describe the hyper-parameters used for the architecture of our algorithm. Since our goal is to ensure that the agents make their decisions as quickly as possible, we do not over-parameterize the network architecture and we use a relatively small network for training purposes. Our algorithm trains a DQN with one input layer, three hidden layers, and one output layer. The hidden layers have 200, 100, and 40 neurons, respectively. We have 7 DQN input ports reserved for the local information feature group explained in Section IV-C. The cardinality constraint on the neighbor sets c is 5 agents. Hence, again from Section IV-C, the input ports reserved for the interferer and the interfered neighbors are $6c = 30$ and $4c = 20$, respectively. This makes a total of 57 DQN input ports reserved for the state set. (We also normalize the DQN inputs with some constants depending on P_{\max} , maximum intra-cell path loss, etc., to optimize the performance.) We use ten discrete power levels, $|A| = 10$. Thus, the DQN has ten outputs. Initial weights of the DQN are generated with the truncated normal distribution function of the TensorFlow, and the activation function is hyperbolic tangent (tanh). Memory parameters at the network trainer, M_b and M_m , are 256 and 1000 samples, respectively. We use the RMSProp algorithm [29] with an adaptive learning rate $\alpha^{(t)}$. For a more stable deep Q-learning outcome, the learning rate is reduced as $\alpha^{(t+1)} = \lambda\alpha^{(t)}$, where $\lambda \in (0, 1)$ is the decay rate of $\alpha^{(t)}$ [30]. Here, $\alpha^{(0)}$ is 5×10^{-3} and λ is 10^{-4} . We also apply adaptive ϵ -greedy algorithm: $\epsilon^{(0)}$ is initialized to 0.2 and it follows $\epsilon^{(t+1)} = \max \{\epsilon_{\min}, \lambda_{\epsilon}\epsilon^{(t)}\}$, where $\epsilon_{\min} = 10^{-2}$ and $\lambda_{\epsilon} = 10^{-4}$. Further, T_u is 100 time slots. Although the discount factor γ is nearly arbitrarily chosen to be close to 1 and increasing γ potentially improves the outcomes of deep Q-learning for most of its applications [30], we set γ to 0.5. The reason we use a moderate level of γ is that the

correlation between agent's actions and its future rewards tends to be smaller for our application due to fading.

We empirically validate the functionality of our algorithm. Hence, each result in this paper is an average of at least 10 randomly initialized simulations. We have two main phases for the simulations: training and testing. Each training lasts 40,000 time slots or $40,000 \times 20 \text{ ms} = 800$ seconds, and each testing lasts 5,000 time slots or 100 seconds. During the testing, our algorithm terminates the ϵ -greedy algorithm and the training of DQN.

We have five benchmarks to evaluate the performance of our algorithm. The first two benchmarks are 'ideal WMMSE' and 'ideal FP' which are the outcomes of the centralized algorithms introduced in Section III with an assumption of instantaneously acquired full CSI and the centralized algorithm outcome. We use these unrealistic scenarios as benchmarks to compare our algorithm's handiness in realistic situations with delayed CSI. The third benchmark is the 'central power allocation' (central), where we introduce one time slot delay on the full CSI and feed it to the FP algorithm. Even the single time slot delay to acquire the full CSI is a generous assumption, but it is a useful approach to reflect potential performance of negligible computation time achieved with the supervised learning approach introduced in [9]. The next benchmark is the 'random' allocation, where each agent chooses its transmit power for each slot at random uniformly between 0 and P_{\max} . The last benchmark is the 'full-power' allocation, i.e., each agent's transmit power is P_{\max} for all slots.

B. Sum-Rate Maximization

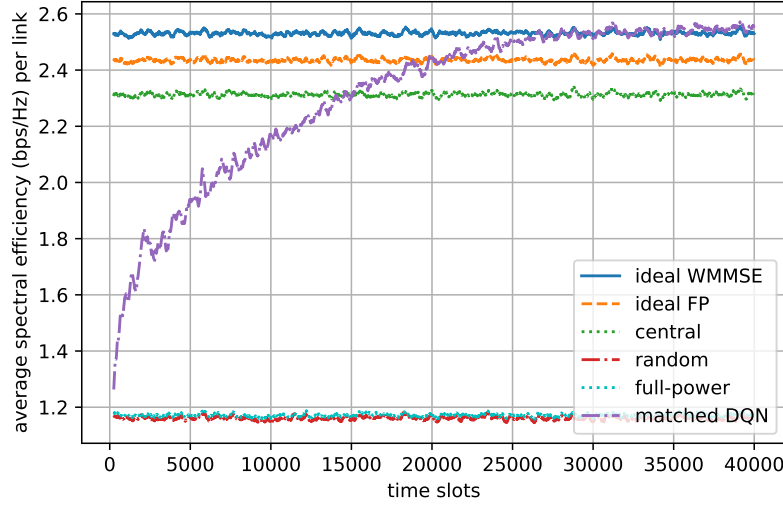
In this section, we analyze the sum-rate performance of our algorithm. Therefore, all weights of the network agents are equal to 1 through all time slots.

1) *Robustness*: Our main objective here is to show our algorithm is robust with respect to the initial receiver placement and network initialization parameters like R and r . In this section, there are always $n = 19$ links.

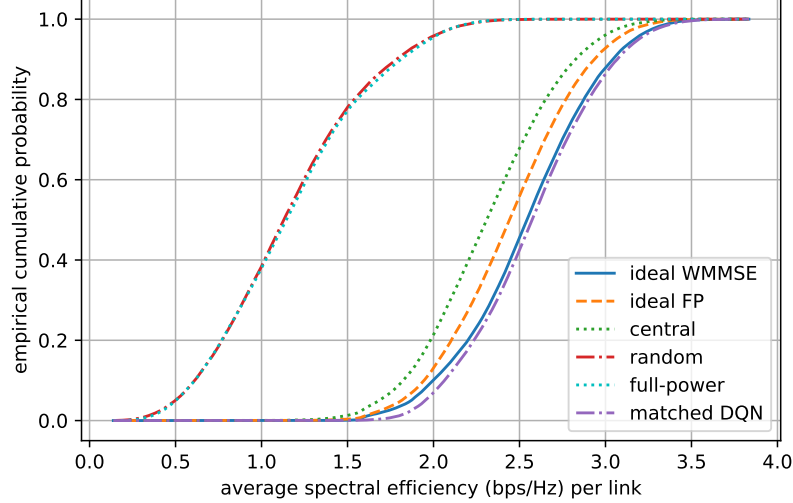
TABLE I: Testing results with variant variant half transmitter-to-transmitter distance. $n = 19$ links, $r = 10$ m, $f_d = 10$ Hz.

R (m)	average sum-rate performance in bps/Hz per link							
	DQN		benchmark power allocations					
	matched	unmatched	WMMSE	FP	central	random	full-power	
100	2.88	2.67	2.97	2.87	2.67	1.76	1.80	
300	2.82	2.54	2.79	2.68	2.54	1.43	1.45	
400	2.52	2.26	2.49	2.39	2.25	1.10	1.11	
500	2.56	2.27	2.48	2.39	2.26	1.01	1.02	
1000	2.57	2.29	2.53	2.44	2.32	1.16	1.17	

We use two approaches to evaluate the performance of our algorithm. The first approach is the ‘matched’ DQN where we use the first 40,000 time slots to train a DQN from scratch, whereas for the ‘unmatched’ DQN we ignore the matched DQN specialized for this specific initialization and for the testing (the last 5,000 time slots) we randomly pick another DQN trained for another initialization. Hence, the unmatched DQN approach is a handy tool to evaluate the robustness of our DQN with respect to network topology and channel variations. The testing results with variant R are demonstrated in Table I. We see that training a DQN from scratch for the specific initialization is able to outperform both state-of-the-art centralized algorithms. Interestingly, the unmatched DQN approach converges to the central power allocation where we feed the FP algorithm with delayed full CSI. Our algorithm is able to handle the changes in network initialization and performs as good as the FP algorithm with delayed CSI feedback. The DQN approach achieves this performance with distributed execution and incomplete CSI. In addition, training a DQN from scratch enables our algorithm to learn to compensate for CSI delays. By using only the available local information, our algorithm outperforms the centralized state-of-the-art algorithms that are under ideal conditions. Although training a DQN from scratch swiftly converges in about 25,000 time slots (shown in Fig. 4a), using the weights of a previously trained DQN as the initialization of training could speed



(a) Training - Moving average spectral efficiency per link of previous 250 time slots.



(b) Testing - Empirical CDF.

Fig. 4: Sum-rate maximization. $n = 19$ links, $R = 1000$ m, $r = 10$ m, $f_d = 10$ Hz.

up the convergence even more.

We conclude this section by showing the results of additional simulations with r and f_d taken as variables, summarized in Table II and Table III, respectively. As the area of receiver-free inner region increases, the receivers get closer to the interfering transmitters and the interference mitigation becomes more necessary. Hence, the random and full-power allocations tend to show much lower sum-rate performance compared to the central algorithms. For that case, our algorithm still shows decent performance and

TABLE II: Testing results with variant inner region radius. $n = 19$ links, $R = 500$ m, $f_d = 10$ Hz.

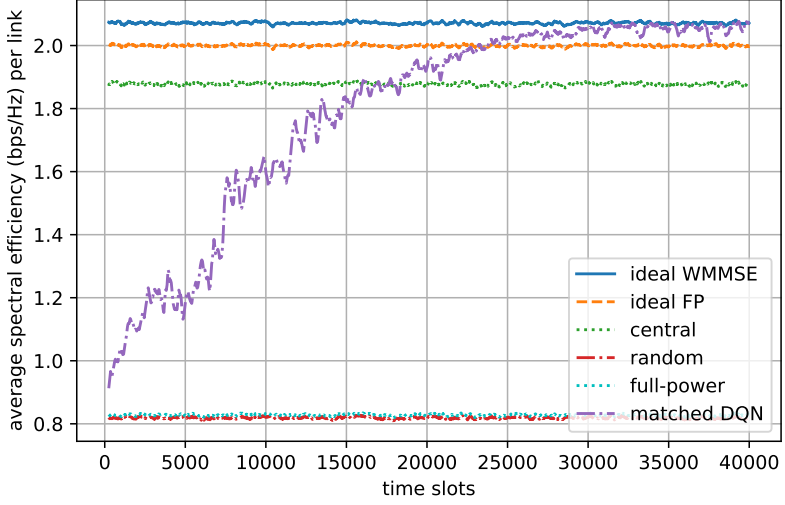
r (m)	average sum-rate performance in bps/Hz per link							
	DQN		benchmark power allocations					
	matched	unmatched	WMMSE	FP	central	random	full-power	
10	2.56	2.27	2.48	2.39	2.26	1.01	1.02	
200	2.16	1.79	2.08	1.99	1.86	0.71	0.71	
400	2.13	1.85	2.01	1.93	1.80	0.55	0.55	
499	1.87	1.59	1.83	1.77	1.65	0.39	0.38	

TABLE III: Testing results with variant maximum Doppler frequency. $n = 19$ links, $R = 500$ m, $r = 10$ m. ('random' means f_d of each link is randomly picked between 2 Hz and 15 Hz for each time slot t .)

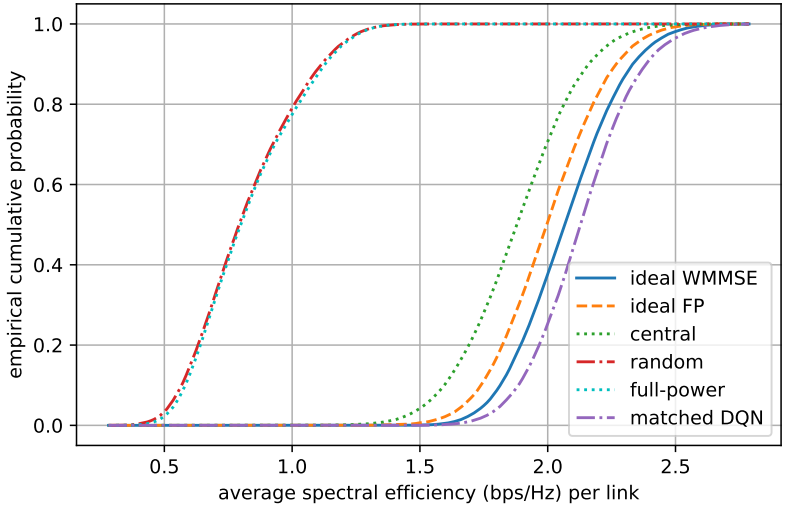
f_d (Hz)	average sum-rate performance in bps/Hz per link							
	DQN		benchmark power allocations					
	matched	unmatched	WMMSE	FP	central	random	full-power	
2	2.72	2.56	2.58	2.47	2.46	1.20	1.21	
5	2.63	2.30	2.49	2.39	2.34	0.90	0.89	
10	2.56	2.27	2.48	2.39	2.26	1.01	1.02	
15	2.65	2.25	2.54	2.43	2.26	1.05	1.05	
random	2.85	2.59	2.82	2.70	2.59	1.40	1.42	

the convergence rate is still about 25,000 time slots. We also stressed the DQN under various f_d scenarios. As we reduce f_d , its sum-rate performance remains unchanged, but the convergence time drops to 15,000 time slots. When f_d becomes 15 Hz, the convergence time increases to 30,000 time slots. Intuitively, the reason of this effect on the convergence rate is that the variation of states visited during the training phase is proportional to f_d .

2) *Scalability*: In the previous subsection, we considered some network initializations with just 19 links. Now, we increase the total number of links to show the scalability of our algorithm. Fig. 5 shows that as we increase n to 50 links, the DQN still converges in 25,000 time slots with high sum-rate performance.



(a) Training - Moving average spectral efficiency per link of the previous 250 time slots.



(b) Testing - Empirical CDF.

Fig. 5: Sum-rate maximization. $n = 50$ links, $R = 500$ m, $r = 10$ m, $f_d = 10$ Hz.

As we keep on increasing n to 100 links, from Table IV, the DQN sum-rate performance becomes lower than the performance of both centralized algorithms. This is because of the fixed input architecture of the DQN (the limitation c on the number of neighbors fed into the DQN). Each agent only considers $c = 5$ interferer and interfered neighbors. The performance of DQN can be improved for that case by increasing c , but there is a trade-off between c and the complexity of network architecture.

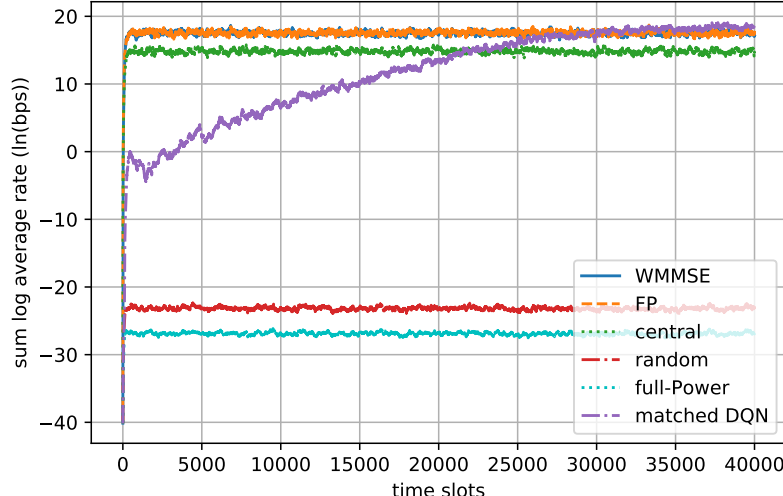
TABLE IV: Testing results with variant total number of links. $R = 500$ m, $r = 10$ m, $f_d = 10$ Hz.

n (links)	average sum-rate performance in bps/Hz per link							
	DQN		benchmark power allocations					
	matched	unmatched	WMMSE	FP	central	random	full-power	
19	2.56	2.27	2.48	2.39	2.26	1.01	1.02	
50	2.13	2.00	2.07	2.00	1.88	0.82	0.83	
100	1.64	1.58	1.75	1.69	1.56	0.64	0.64	

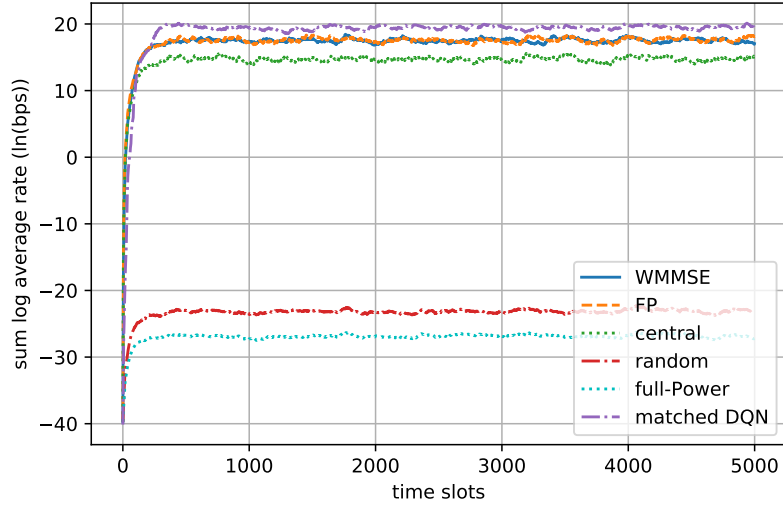
It is worth pointing out that each agent is able to determine its own action approximately between 0.2 ms and 0.3 ms with our algorithm. Therefore, our algorithm matches with the concept of dynamic power allocation. In addition, running a single batch takes about 13 to 17 ms. This is again feasible, since T is taken 20 ms. Most importantly, because of the fixed architecture of the DQN, increasing the total number of links from 19 to 100 has no impact on these values. It will just increase the queue memory in the network trainer, which is maintainable. However, the centralized iterative algorithms are not scalable. For the FP algorithm it takes about 15 ms to converge for $n = 19$ links, but with $n = 100$ links it becomes 35 ms. The WMMSE algorithm converges slightly slower, and the convergence time is still proportional to n which limits its scalability.

C. Proportionally Fair Scheduling

In this section, we change the link weights according to (7) to ensure fairness as described in Section III. We choose the β term in (8) to be 0.01. The objective of proportional fair scheduling is maximizing the sum log-average rate of all links given in (8). Therefore, we use convergence to this objective as performance-metric of the DQN for proportional fair scheduling. We also make some additions to the training and testing stage of DQN. We need an initialization for the link weights. This is done by letting all transmitters to serve their receivers with full-power at $t = 0$, and initialize weights according to the initial spectral efficiencies computed from (4). We do similar thing for the testing stage, too. In order to



(a) Training.



(b) Testing.

Fig. 6: Proportionally fair scheduling. $n = 19$ links, $R = 500$ m, $r = 10$ m, $f_d = 10$ Hz.

see the performance of the trained DQN from scratch, we reinitialize the weights after the first 40,000 slots.

The convergence of DQN for proportional fair scheduling is shown in Fig. 6. Again, the training stage converges to a desirable scheduling in about 25,000 time slots. Once the network is trained, as we reinitialize the link weights, our algorithm converges to an optimal scheduling in a distributed fashion as fast as the centralized algorithms. Next, we set R and r as variables to get results in Table V and Table

TABLE V: Proportional fair scheduling with variant half transmitter-to-transmitter distance. $n = 19$ links, $r = 10$ m, $f_d = 10$ Hz.

R (m)	convergence of the network sum log-average rate (ln (bps))							
	DQN		benchmark power allocations					
	matched	unmatched	WMMSE	FP	central	random	full-power	
100	27.45	25.45	29.98	29.58	26.53	16.37	15.60	
300	22.38	21.65	22.68	22.21	19.61	-7.96	-10.68	
400	22.95	21.70	23.02	22.96	20.45	-10.00	-12.74	
500	19.55	18.74	17.52	17.72	14.80	-22.99	-26.77	
1000	16.25	12.86	14.11	13.98	11.27	-27.08	-30.72	

TABLE VI: Proportional fair scheduling with variant inner region radius. $n = 19$ links, $R = 500$ m, $f_d = 10$ Hz.

r (m)	convergence of the network sum log-average rate (ln (bps))							
	DQN		benchmark power allocations					
	matched	unmatched	WMMSE	FP	central	random	full-power	
10	19.55	18.74	17.52	17.72	14.80	-22.99	-26.77	
200	19.24	17.33	16.74	16.74	14.10	-24.61	-28.32	
400	16.37	14.76	15.11	14.89	11.99	-37.35	-41.41	
499	13.51	12.44	12.07	12.12	9.26	-43.45	-47.78	

VI. We see that the trained DQN from scratch still outperforms the centralized algorithms in most of the initializations, using the unmatched DQN also achieves a high performance similar to the previous sections.

VI. CONCLUSION AND FUTURE WORK

In this paper, we have proposed a distributed model-free power allocation algorithm which achieves comparable performance with existing state-of-the-art centralized algorithms. We see a great potential in

applying the reinforcement learning techniques on various dynamic wireless network resource management tasks in place of the optimization techniques. The proposed approach returns the new suboptimal power allocation much quicker than two of the popular centralized algorithms taken as the benchmarks in this paper. In addition, by using the limited local CSI and some realistic practical constraints, our deep Q-learning approach usually outperforms the generic WMMSE and FP algorithms which requires the full CSI which is an inapplicable condition. In future work, we plan to add multiple associated receivers per transmitter and consider multiple frequency bands. Although the centralized training phase seems to be a limitation on the proposed algorithm, we showed a jump-start on the training of DQN can be implemented by using initial weights of another DQN previously trained for a different setup. We plan to work more on this observation. Finally, we used global training in this paper, whereas reinitializing a local training over the regions where new links joined or performance dropped under a certain threshold is also an interesting direction to consider.

VII. ACKNOWLEDGEMENT

We thank Mingyi Hong and Wei Yu for stimulating discussions.

REFERENCES

- [1] M. Chiang, P. Hande, T. Lan, and C. W. Tan, “Power control in wireless cellular networks,” *Foundations and Trends in Networking*, vol. 2, no. 4, pp. 381–533, 2007.
- [2] Z. Q. Luo and S. Zhang, “Dynamic spectrum management: Complexity and duality,” *IEEE Journal of Selected Topics in Signal Processing*, vol. 2, pp. 57–73, Feb 2008.
- [3] Q. Shi, M. Razaviyayn, Z. Q. Luo, and C. He, “An iteratively weighted mmse approach to distributed sum-utility maximization for a mimo interfering broadcast channel,” *IEEE Transactions on Signal Processing*, vol. 59, pp. 4331–4340, Sept 2011.
- [4] K. Shen and W. Yu, “Fractional programming for communication systems, Part I: power control and beamforming,” *submitted*, 2017.
- [5] I. Sohn, “Distributed downlink power control by message-passing for very large-scale networks,” *International Journal of Distributed Sensor Networks*, vol. 11, no. 8, p. 902838, 2015.
- [6] J. Huang, R. A. Berry, and M. L. Honig, “Distributed interference compensation for wireless networks,” *IEEE Journal on Selected Areas in Communications*, vol. 24, pp. 1074–1084, May 2006.

- [7] S. G. Kiani, G. E. Oien, and D. Gesbert, “Maximizing multicell capacity using distributed power allocation and scheduling,” in *2007 IEEE Wireless Communications and Networking Conference*, pp. 1690–1694, March 2007.
- [8] H. Zhang, L. Venturino, N. Prasad, P. Li, S. Rangarajan, and X. Wang, “Weighted sum-rate maximization in multi-cell networks via coordinated scheduling and discrete power control,” *IEEE Journal on Selected Areas in Communications*, vol. 29, pp. 1214–1224, June 2011.
- [9] H. Sun, X. Chen, Q. Shi, M. Hong, X. Fu, and N. D. Sidiropoulos, “Learning to optimize: Training deep neural networks for wireless resource management,” *CoRR*, vol. abs/1705.09412, 2017.
- [10] M. J. Neely, E. Modiano, and C. E. Rohrs, “Dynamic power allocation and routing for time-varying wireless networks,” *IEEE Journal on Selected Areas in Communications*, vol. 23, pp. 89–103, Jan 2005.
- [11] V. Mnih, K. Kavukcuoglu, D. Silver, A. A. Rusu, J. Veness, M. G. Bellemare, A. Graves, M. Riedmiller, A. K. Fidjeland, G. Ostrovski, *et al.*, “Human-level control through deep reinforcement learning,” *Nature*, vol. 518, no. 7540, pp. 529–533, 2015.
- [12] L. Liang, J. Kim, S. C. Jha, K. Sivanesan, and G. Y. Li, “Spectrum and power allocation for vehicular communications with delayed csi feedback,” *IEEE Wireless Communications Letters*, vol. 6, pp. 458–461, Aug 2017.
- [13] M. Bennis and D. Niyato, “A q-learning based approach to interference avoidance in self-organized femtocell networks,” in *2010 IEEE Globecom Workshops*, pp. 706–710, Dec 2010.
- [14] M. Simsek, A. Czylwik, A. Galindo-Serrano, and L. Giupponi, “Improved decentralized q-learning algorithm for interference reduction in lte-femtocells,” in *2011 Wireless Advanced*, pp. 138–143, June 2011.
- [15] R. Amiri, H. Mehrpouyan, L. Fridman, R. K. Mallik, A. Nallanathan, and D. Matolak, “A machine learning approach for power allocation in hetnets considering qos,” *CoRR*, vol. abs/1803.06760, 2018.
- [16] E. Ghadimi, F. D. Calabrese, G. Peters, and P. Soldati, “A reinforcement learning approach to power control and rate adaptation in cellular networks,” in *2017 IEEE International Conference on Communications (ICC)*, pp. 1–7, May 2017.
- [17] F. D. Calabrese, L. Wang, E. Ghadimi, G. Peters, and P. Soldati, “Learning radio resource management in 5g networks: Framework, opportunities and challenges,” *CoRR*, vol. abs/1611.10253, 2016.
- [18] D. N. C. Tse and P. Viswanath, *Fundamentals of Wireless Communication*. Cambridge University Press, 2005.
- [19] L. P. Kaelbling, M. L. Littman, and A. W. Moore, “Reinforcement learning: A survey,” *CoRR*, vol. cs.AI/9605103, 1996.
- [20] R. S. Sutton and A. G. Barto, *Reinforcement Learning: An Introduction*. Cambridge, MA: MIT Press, 1998.
- [21] S. Singh, T. Jaakkola, M. L. Littman, and C. Szepesvári, “Convergence results for single-step on-policy reinforcement-learning algorithms,” *Machine learning*, vol. 38, no. 3, pp. 287–308, 2000.
- [22] A. Galindo-Serrano and L. Giupponi, “Distributed q-learning for interference control in ofdma-based femtocell networks,” in *2010 IEEE 71st Vehicular Technology Conference*, pp. 1–5, May 2010.
- [23] O. Naparstek and K. Cohen, “Deep multi-user reinforcement learning for dynamic spectrum access in multichannel wireless networks,” *CoRR*, vol. abs/1704.02613, 2017.
- [24] Y. LeCun, Y. Bengio, and G. Hinton, “Deep learning,” *Nature*, vol. 521, pp. 436 EP –, May 2015.

- [25] H. Ye and G. Y. Li, “Deep reinforcement learning for resource allocation in V2V communications,” *CoRR*, vol. abs/1711.00968, 2017.
- [26] Y. Yu, T. Wang, and S. C. Liew, “Deep-reinforcement learning multiple access for heterogeneous wireless networks,” *CoRR*, vol. abs/1712.00162, 2017.
- [27] “Requirements for further advancements for E-UTRA (LTE-Advanced).” 3GPP TR 36.913 v.8.0.0, available at <http://www.3gpp.org>.
- [28] B. Zhuang, D. Guo, and M. L. Honig, “Energy-efficient cell activation, user association, and spectrum allocation in heterogeneous networks,” *IEEE Journal on Selected Areas in Communications*, vol. 34, pp. 823–831, April 2016.
- [29] S. Ruder, “An overview of gradient descent optimization algorithms,” *CoRR*, vol. abs/1609.04747, 2016.
- [30] V. François-Lavet, R. Fonteneau, and D. Ernst, “How to discount deep reinforcement learning: Towards new dynamic strategies,” *CoRR*, vol. abs/1512.02011, 2015.